ARTICLE

Electroless Deposition of Nickel Nanowire and Nanotube Arrays as Supports for Pt-Pd Catalyst for Ethanol Electrooxidation

Pei-xia Yang[a*], Jie Zhang[a], Lei Liu[b], Mao-zhong An[a]

a. School of Chemical Engineering and Technology, Harbin Institute of Technology, Harbin 150001, China

b. China Automotive Technology and Research Center, Tianjin 300300, China

(Dated: Received on December 3, 2014; Accepted on January 26, 2015)

Nickel nanowire and nanotube arrays as supports for Pt-Pd catalyst were prepared by electroless deposition with anodic aluminum oxide template. Pt-Pd composite catalyst was deposited on the arrays by displacement reaction. SEM images show that the nickel nanowires have an average diameter of 100 nm and the nickel nanotubes have an average inner diameter of 200 nm. EDS scanning reveals that elemental Pt and Pd disperse uniformly on the arrays. Cyclic voltammetry study indicates that the nickel nanotube array loaded with Pt-Pd possesses a higher electrochemical activity for ethanol oxidation than the nickel nanowire array with Pt-Pd.

Key words: Pt-Pd catalyst, Anodic aluminum oxide template, Nanomaterials, Electroless deposition, Energy storage and conversion

I. INTRODUCTION

Ethanol, as one kind of alcohol liquid fuel, has been investigated widely in recent years because of its low toxicity and abundant raw materials [1]. Catalysts based on Pt and Pd are recognized as the best [2] and have been extensively studied for ethanol electrooxidation [3]. However, Pt and Pd have a limited supply and high cost [4]. Increasing studies are focused on the development of the supports for Pt and Pd catalysts [5, 6]. Carbon supported Pt and Pt-based alloys are investigated widely as the electrocatalysts for the oxidation of methanol and ethanol [6, 7], but they are faced with substantial problems, such as the low electrocatalytic activity for the alcohol oxidation [8]. Nanostructure materials as the catalyst or the supports of the catalysts have intrinsic advantages due to their extremely high surface-to-volume ratios [8]. Anodic aluminum oxide (AAO) template is versatile for preparing nanostructures [9−11]. Pt nanotube array (NTA) and Pd nanowire array (NWA), as the catalysts for ethanol electrooxidation, have been electrodeposited with AAO template [8, 12]. Whereas electrodeposition has some drawbacks in the manipulation, for example, a metal film have to be deposited on one side of the template in advance [13]. Electroless deposition can overcome the deficiency, as reported that nickel NTA has been prepared by electroless deposition with AAO template [13].

In the present work, nickel NWA and NTA were fabricated by electroless deposition with AAO template. The electrocatalytic activity of Pt-Pd composite catalyst, deposited on the arrays by displacement reaction, has been investigated for ethanol electrooxidation in alkaline media.

II. EXPERIMENTS

The nickel NWA and NTA were prepared by electroless nickel deposition with AAO template. Firstly, sensitization and activation were carried out at 25 °C for 1 min in the solution of 0.3wt%$SnCl_2$+2.5wt%HCl, and in the solution of 0.1wt%$PdCl_2$+1wt%HCl, respectively. Then electroless nickel deposition was realized in the solution composed of 20 g/L $NiSO_4$, 25 g/L NaH_2PO_2, and 2 μg/mL $Pb(NO_3)_2$ at pH=4−5 and 70 °C. Subsequently, a nickel layer was electrodeposited on one side of the template to support the NWA or NTA when the AAO template was removed. Lastly, the AAO template was dissolved in 2 mol/L NaOH solution, which produced the free-standing nickel NWA or NTA. Pt and Pd were simultaneously deposited on the two arrays by the single-displacement reaction between nickel metal and the solution consisting of chloroplatinic acid and palladium chloride.

The morphology of nickel NWA and NTA was observed by scanning electron microscopy (SEM, KYKY-EM3200). The electrochemical measurements were performed in a typical three-electrode cell with the calomel electrode (Hg/Hg_2Cl_2) as the reference electrode and a platinum sheet as the counter electrode. The working electrode has a macroscopic area of 0.1 cm^2. All the nickel support, electrodeposited before removing

*Author to whom correspondence should be addressed. E-mail: yangpeixia@hit.edu.cn, Tel./FAX: +86-451-86418616

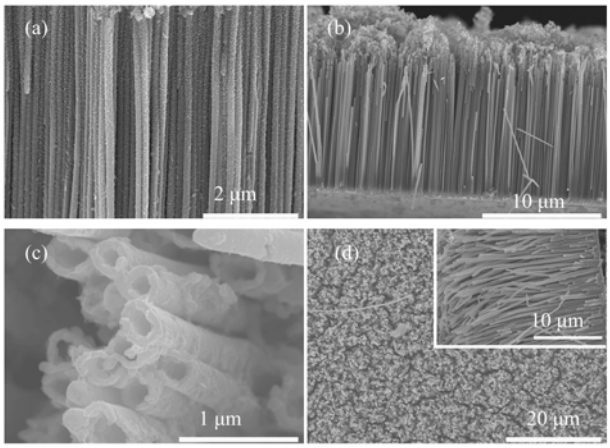

FIG. 1 SEM images of the nickel NWA (a, b) and NTA (c, d) prepared by electroless deposition in the AAO templates with pore sizes of about 100 and 250 nm, respectively.

AAO template, on the working electrode was covered by epoxy resin, in order to make only NTA or NWA be exposed to the electrolyte. The electrolyte used for the measurements was 1 mol/L KOH solution or the solution of 1 mol/L KOH+1 mol/L C_2H_5OH. Argon gas was pumped into the solutions for 30 min before each experiment.

III. RESULTS AND DISCUSSION

The deposition procedure of nickel metal in the AAO template is similar to that reported by Li *et al.* [14]. After submerging activated AAO template with throughhole into the electroless bath, nickel first nucleates on the Pd active sites and then the nucleuses grow to form a layer covering the inner wall of the holes. The formation of nickel nanowires or nanotubes is controlled by the pore size of the AAO template used and the deposition time. Small pore size combined with long deposition time advantages the formation of nanowire. As displayed in Fig.1 (a) and (b), highly ordered nickel nanowires with an average diameter of 100 nm were produced. The template used had an average pore size of 100 nm, and the deposition time was 40 min. The nanowires with the average height of 15 μm can freestand together as an array, which indicates that the wires possess a good mechanical strength. On the other hand, relatively large pore size combined with short deposition time results in the formation of nanotubes. The AAO template with a pore size of about 250 nm was used to construct the nickel NTA, whose SEM images are shown in Fig.1 (c) and (d). The deposition time was 30 min. The uniform nickel nanotubes have an average inner diameter of 200 nm and a wall thickness of about 50 nm. The height of the NTA is about 20 μm, exhibited in the inset of Fig.1(d). At the edge of the array, there are some broken nanotubes caused in the preparation process of the sample.

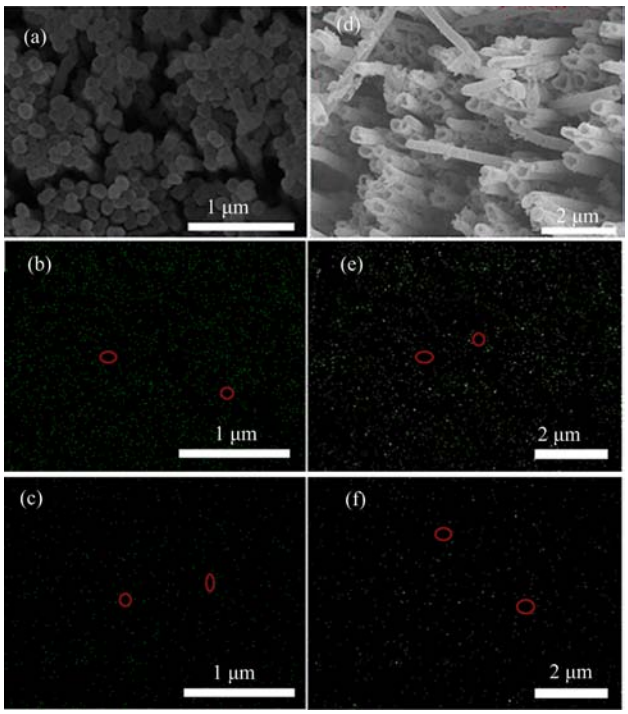

FIG. 2 EDS scanning results of Pd and Pt deposited on the surface of (a) the nickel NWA and (d) nickel NTA. (b) Pd and (c) Pt on the nickel nanowires. (e) Pd and (f) Pt on the nickel nanotubes.

The Pd and Pt were simultaneously deposited on the two arrays by simply submerging the NWA and NTA into the solution of 0.1 g/L H_2PtCl_6+0.04 g/L $PdCl_2$ for 5 min. Both arrays keep its original morphology after depositing Pd and Pt on them as displayed in Fig.2 (a) and (d). Figure 2 shows the EDS scanning results of Pd and Pt deposited on the surface of the nickel NWA and NTA. The bright green dots, representing the detected metallic element, disperse uniformly on both arrays. The small circles (see the red circles in Fig.2 (b), (c), (e), (f)) were caused by the quicker displacement reaction at the top edge of the nickel NWA or NTA. In addition, the density of the bright dots in Fig.2 (b) and (e) for Pd is obviously larger than that in Fig.2 (c) and (f) for Pt, which indicates more Pd was deposited on both arrays, although the $PdCl_2$ has a lower concentration than that of H_2PtCl_6 in the solution. This result may be attributed to two reasons: (i) the different numbers of electrons between the two displacement reactions, (ii) the residual Pd in the activation process before the electroless nickel deposition.

Cyclic voltammetry of the nickel NWA and NTA loaded with Pt-Pd was measured in 1 mol/L KOH solution and in 1 mol/L KOH+1 mol/L C_2H_5OH solution. Figure 3 shows the cyclic voltammograms obtained from the two solutions. The Pt-Pd composite catalyst on both arrays was deposited in the same condition as de-

DOI:10.1063/1674-0068/28/cjcp1412204

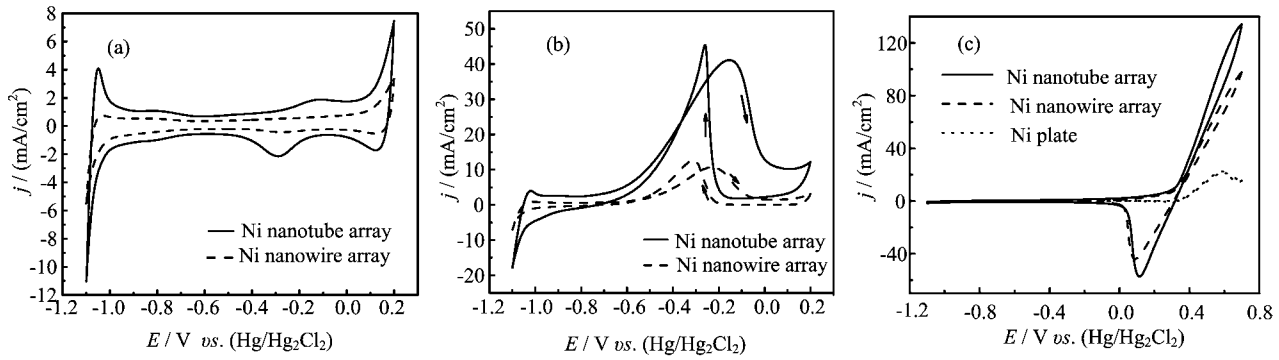

FIG. 3 Cyclic voltammograms of the nickel NWA and NTA with Pt-Pd (a) in 1 mol/L KOH solution, and (b) in 1 mol/L KOH+1 mol/L C_2H_5OH solution. (c) Cyclic voltammograms of the nickel plate, NWA, and NTA.

scribed previously. The potential scan with a rate of 50 mV/s ranges from −1.10 V to 0.20 V *vs.* Hg/Hg_2Cl_2. In this potential range no anodic peak appears in the cyclic voltammograms of the nickel plate, nanowire, and nanotube in 1 mol/L KOH+1 mol/L C_2H_5OH solution (see Fig.3(c)). The humps between −0.70 and −1.10 V in the cyclic voltammograms of the two array electrodes (Fig.3(a)) result from the desorption of atomic hydrogen on the Pt-Pd composite catalyst. The coulombic charge for hydrogen desorption (Q_H) corresponds to the area of the humps with reduction of the double layer region, and is proportional to the electrochemically active area of the catalysts [15]. The nickel NTA electrode has a Q_H of 5.90 mC/cm^2 larger than that of 1.35 mC/cm^2 of the nickel NWA electrode, most likely due to different structures between the two arrays. According to Fig.3(b), the onset potential (where the current density reaches 10% of anodic peak current density [16]) of the ethanol oxidation on the NTA array electrode with Pt-Pd is −0.65 V, which is 50 mV more negative than that on the NWA array electrode (−0.60 V). Meanwhile, the voltammogram on NTA has a four times higher anodic peak current density (41.24 mA/cm^2) than that (10.06 mA/cm^2) on NWA. These results demonstrate that nickel NTA loaded with Pt-Pd shows a much higher activity than nickel NWA with Pt-Pd in alkaline media.

IV. CONCLUSION

Highly ordered nickel NWA and NTA were fabricated by electroless deposition with AAO template. The nickel nanowires have an average diameter of 100 nm, and the nickel nanotubes have an average inner diameter of 200 nm. The Pd and Pt were simultaneously deposited on the arrays by simply submerging the NWA and NTA into the solution with 0.1 g/L H_2PtCl_6+ 0.04 g/L $PdCl_2$. EDS scanning results reveal that Pd and Pt disperse uniformly on the two arrays. The nickel NTA with Pb-Pt has a higher electrochemical activity than the nickel NWA loaded with Pb-Pt.

V. ACKNOWLEDGMENTS

This work was supported by the Fundamental Research Funds for the Central Universities (No.HIT.ICRST.2010005).

[1] M. Y. Wang, J. H. Chen, Z. Fan, H. Tang, G. H. Deng, D. L. He, and Y. F. Kuang, Carbon **42**, 3257 (2004).
[2] B. C. H. Steele and A. Heinzel, Nature **414**, 345 (2001).
[3] S. Song and P. Tsiakaras, Appl. Catal. B **63**, 187 (2006).
[4] F. Bensebaa, A. A. Farah, D. Wang, C. Bock, X. Du, J. Kung, and Y. Le Page, J. Phys. Chem. B **109**, 15339 (2005).
[5] M. Gustavsson, H. Ekström, P. Hanarp, L. Eurenius, G. Lindbergh, E. Olsson, and B. Kasemo, J. Power Sources **163**, 671 (2007).
[6] C. Xu, L. Cheng, P. Shen, and Y. Liu, Electrochem. Commun. **9**, 997 (2007).
[7] Y. Lee, S. Kim, J. Kim, and S. Lee, Mater. Lett. **123**, 184 (2014).
[8] X. Zhang, D. Dong, D. Li, T. Williams, H. Wang, and P. A. Webley, Electrochem. Commun. **11**, 190 (2009).
[9] J. C. Hulteen and C. R. Martin, J. Mater. Chem. **7**, 1075 (1997).
[10] C. R. Martin, Science **266**, 1961 (1994).
[11] X. Chen, X. J. Huang, J. R. Huang, Z. Y. Huang, W. H. Xu, and J. H. Liu, Chin. J. Chem. Phys. **19**, 79 (2006).
[12] C. W. Xu, H. Wang, P. K. Shen, and S. P. Jiang, Adv. Mater. **19**, 4256 (2007).
[13] W. Wang, N. Li, X. Li, W. Geng, and S. Qiu, Mater. Res. Bull. **41**, 1417 (2006).
[14] Q. Q Li, S. S. Fan, W. Q. Han, C. H. Sun, and W. J. Liang, Jpn. J. Appl. Phys. **36**, L501 (1997).
[15] A. Pozio, M. De Francesco, A. Cemmi, F. Cardellini, and L. Giorgi, J. Power Sources **105**, 13 (2002).
[16] F. Maillard, A. Bonnefont, M. Chatenet, L. Guétaz, B. Doisneau-Cottignies, H. Roussel, and U. Stimming, Electrochim. Acta **53**, 811 (2007).

DOI:10.1063/1674-0068/28/cjcp1412204